터널과 지하공간, 한국암반공학회
Vol. 13, No. 2, 2003, pp. 117~124

TUNNEL & UNDERGROUND Vol. 13, No. 2, 2003, pp. 117-124
J. of Korean Society for Rock Mech.

Influence of Rock Inhomogeneity on the Static Tensile Strength of Rock

Sang Ho Cho[1], Hyung Sik Yang[2] and Katsuhiko Kaneko[1]

암석의 정적 인장강도에 미치는 불균질성의 영향

조상호 · 양형식 · 金子 勝比古

Abstract. The fracture processes under static tensile loading were simulated using a proposed numerical simulation method, based on finite element method and fracture mechanism, and analyzed to verify an influence of rock inhomogeneity on static tensile strength. Static tensile strengths for the specimen models with different spatial microscopic tensile strength when m=5 and m=50 were estimated. These analyses revealed that the static tensile strength becomes closer to the mean microscopic tensile strength at a higher uniformity coefficient and the scatter of the strength data decreases in increasing the uniformity coefficients. Therefore, it could be concluded that rock inhomogeneity has an effect on static tensile strength.

KeyWords: Fracture processes, Static tensile loading, Rock inhomogeneity, Static tensile strength, Microscopic tensile strength

초 록. 암석의 불균질성이 정적 인장강도에 미치는 영향을 평가하기 위해, 유한요소해석법과 파괴역학에 기초하여 제안된 수치해석기법을 사용하여 정적 일축인장시험을 가정한 암석 파쇄 과정을 해석하였다. 정적 인장강도는 미시적 인장강도를 가진 모델 시험편의 파쇄 과정으로부터 평가되었으며, 평가된 공시체 강도는 미시적 인장강도의 최소치보다 약간 큰 값에 일치하였으며, 그 강도의 흩어짐은 균질성 계수가 증가함에 따라 감소하였다. 본 해석 결과들로부터 암석 불균질성이 정적 인장강도에 미치는 중요한 요인임을 지적할 수 있었다.

핵심어: 파쇄 과정, 정적 인장하중, 암석 불균질성, 정적 인장강도, 미시적 인장강도

1. Introduction

Rock is less resistant to tension than to compression or shear and tensile behavior of the rock often develops before compression or shear failure. Thus, tensile strength of rock has been considered as important parameter influencing rock deformation and fracture. The tensile strength can be categorized into dynamic and static tensile strength. The static tensile strength is generally measured by Brazilian, uni-axial tension, and point load tests using material tester such as material test systems (MTS) and the dynamic tensile strength is often measured by using the split Hopkinson pressure bar (SHPB) (for example Reinhardt et al., 1986 and Tedesco et al., 1995), the dynamic tensile test (Ma, 1998) based on Hopkinson effect with spalling phenomena, etc. The transition of the dynamic and static tensile strengths exists at the range of 0.1~1 (s^{-1}) in strain rate (Jung et al., 2001).

It is well known that there are significant differences between dynamic and static tensile strength and the tensile strengths increase in increasing stress rate or strain rate. Bacon (1962) determined the dynamic tensile strength of rock using a pendulum to impart energy, in the form of a sharp pulse, to the end of a long core suspended from overhead supports by fine wires. His results showed that the dynamic tensile strength was one to four times the static tensile strength. Rinehart (1965) reported that the dynamic tensile strength was six to ten times the static tensile strength. Birkimer (1970) pointed out that the dynamic tensile strength of rock is not constant

[1] Graduate School of Eng., Hokkaido Univ., Sapporo, Japan
[2] Dep. Geosystem Eng., Chonnam Nat'l Univ., Korea
접수일: 2003년 3월 12일
심사 완료일: 2003년 4월 18일

and varies with the straining rate. Ma (1998) showed that tensile strengths obtained by the technique based on Hopkinson's effect were 1.2 to 3.3 times larger than those obtained with the Brazilian test. Cho et al. (2002) identified the inhomogeneity of the microstructure strength of rocks as a contributing factor to the difference between the static and dynamic tensile strengths.

In this paper, to simulate fracture process in a rock specimen model subjected to static loading in tension, a numerical simulation method, based on finite element method and fracture mechanism, is proposed. In order to verify an influence of inhomogeneity of rock on static tensile strength, static tensile strengths of the specimen models considering the microstructure strength of rock were determined using the proposed simulation method. At the accompanying paper (Cho et al., 2003), an influence of inhomogeneity of rock on dynamic tensile strength is discussed and compared with the static tensile strength.

2. Numerical Simulation Approach

2.1 Microscopic strength of rock

Rock is an inhomogeneous material, and the inhomogeneity plays a significant role in the fracture process. The strength and elastic modulus may be used to model the rock inhomogeneity. The strength of the rock is more sensitive to the fracture process than the elastic modulus. It is therefore reasonable to consider the strength of the rock as a function of the microstructures to account for the inhomogeneity, while using a constant elastic modulus.

Consider a microstructure that consists of a set of k microstructure elements. S_j is the strength of the jth element, and σ_j is the stress in the jth element. The fracture criterion of the microstructure may be described as S_j/σ_j $(j=1\sim k)$. The apparent strength S^*_j of the jth element subjected to a homogeneous stress is $S^*_j=(S_j/\sigma_j)\times\sigma$, where σ is the mean stress in the rock specimen. In this study, the apparent strength S^*_j is treated as a microscopic strength x_t.

Assume that the rock fractures are governed by latent cracks. Weibull's distribution (Weibull, 1951) can be used to account for the microscopic strength. Using Weibull's distribution, the cumulative probability distribution $G(n,x_t)$ and the mean microscopic strength x_t of the nth latent crack are

$$G(n,x_t) = 1 - exp(\alpha x_t^{m_1}) \tag{1}$$

$$x_t(n) = (\alpha n)^{-1/m_1}\Gamma\left(1+\frac{1}{m_1}\right) \tag{2}$$

where Γ is the Gamma function, and α and m_1 are material constants. The cumulative probability distribution $G(V,x_t)$ can be rewritten as

$$G(V,x_t) = 1 - exp\left[-\left(\frac{x_t}{\bar{x}_t(V)}\right)^{m_1}\Gamma^{m_1}\left(1+\frac{1}{m_1}\right)\right] \tag{3}$$

where $\bar{x}_t$ is the mean strength in a volume V. The strength decreases with increasing size due to the existence of cracks or flaws. To consider the size effect, the mean strength $x_t(V)$ in a volume V can be rewritten using the mean strength (V_0) in a reference volume V_0,

$$x_t(V) = \left(\frac{V}{V_0}\right)^{-1/m_2} x_t(V_0) \tag{4}$$

where m_2 is a material constant related to the size effect of the material. The constants m_1 and m_2 with respect to Equations (3) and (4) have been evaluated for various rocks (Kaneko, 1995); m_1 is ranging from 15.2 to 17.4 in Kimachi sandstone and 7.9 to 15.5 in Inada granite, and m_2 is 21.68 in Kimachi sandstone and 18.32 in Inada granite. In this analysis, the relationship between m_2 and m_1 is used as $m_2=2m_1$, here m_1 is defined as the coefficient of uniformity m. Random numbers satisfying Weibull's distribution were generated to give the spatial distribution of the microscopic strengths in the analysis model.

2.2 Numerical simulation method for the fracture process

To simulate the fracture process under static loading, the increment displacement form of a finite element method was used. The Incomplete Choleski Decom-

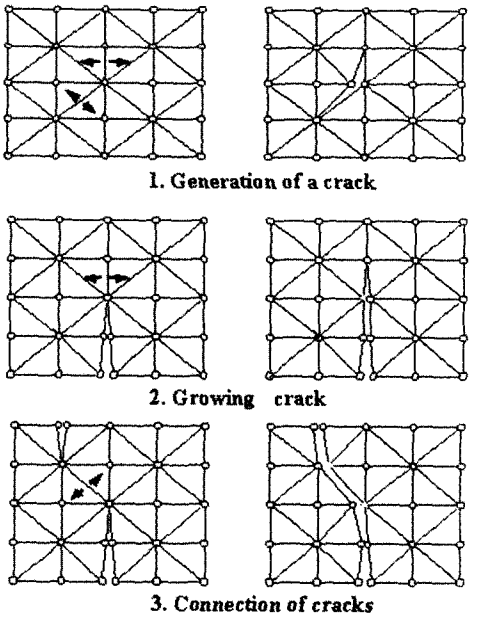

Fig. 1. Remesh process for tensile fracture.

position and Conjugate Gradient (ICCG) method was employed to decrease the required computational memory (Kaneko, 1995). In this analysis, a re-meshing algorithm was used to model the crack propagations, assuming that tensile fractures, *i.e.*, crack initiations, propagations and interconnections, occur at element boundaries as shown in Fig. 1. Thus, the cracks were modeled as separations from the element boundaries without changing the shape of the elements. At each element boundary, the fracture potential was checked at every step. The fracture potential was calculated from the ratio of the normal stress and tensile strength at the element boundary. If the fracture potential of two elements was greater than 1, the node between the elements was separated into two nodes.

In rock fracture mechanics, the behavior of the fracture process zone in front of the crack tips can be simulated with a tensile softening curve (Hillerborg, 1972). Assuming that the mechanical behavior in a fracture process zone during dynamic crack growth is similar to that in static or quasi-static crack growth, the ¼ model (Whittaker et. al, 1992) illustrated in Fig. 2 can be used as the relationship between the crack opening displacement h and the crack bond strength *S*.

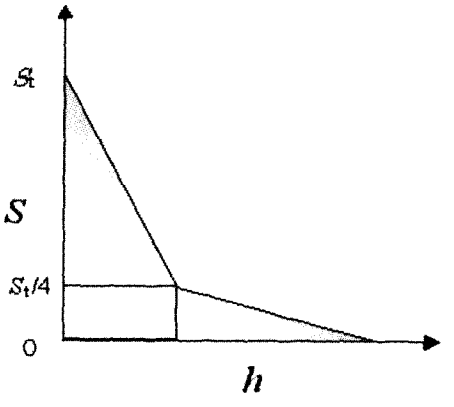

Fig. 2. Tensile softening curve.

To simplify the fracture process, the fracture energy was assigned to zero in this study. Because the cracking and fracture processes were treated as separations of an element, contact problems, *i.e.*, overlapping of the separated elements, may occur due to the perpendicular compression stress that is applied to the separated elements. The problem was solved iteratively to prevent meshing overlaps when the separated elements were in contact with each other. At each iteration, the algorithm checked for crack opening displacements at all of the separated elements. Where these occurred, a contact force was applied until the opening crack displacements became zero.

3. Model Description and Fracture Process Simulation

Brazilian, uni-axial tension, and point load tests are generally used to determine the static tensile strength of rock. In this study, to simulate the fracture process under static loading in direct tension, the uni-axial tension test was modeled and analyzed using the proposed finite element method. The static analysis model is illustrated in Fig. 3, and the parameters and calculation conditions are listed in Table 1. The models were divided into 6000 triangular elements consisting of 3131 nodal points. Random numbers satisfying Weibull's distribution were generated to give the spatial distribution of the microscopic strengths. Figure 4 shows the microscopic tensile strength distributions

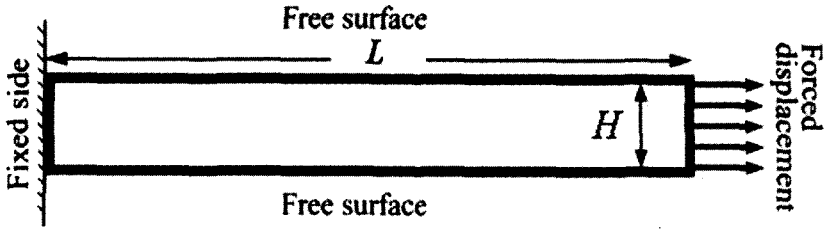

Fig. 3. Geometry of model subjected to static loading.

Table 1. Mechanical properties and calculation conditions for the analysis model.

Parameter	Value
Density ρ (kg/m^3)	2500
Elastic modulus E (GPa)	10
Poisson's ratio ν	0.25
Average compressive strength S_c (MPa)	60
Average tensile strength S_t (MPa)	4.0
Fracture energy G_f (Pa · m)	0
Coefficient of uniformity m	5, 50 and ∞
Time step Δd (μm)	32.56

when m=5 and m=50. Here, the mean tensile strength is 4 MPa, m=5 corresponds to inhomogeneous materials, and m=50 corresponds to comparatively homogeneous materials. The loading condition was simulated by displacement instead of a pressure to observe crack propagations and the specimen behavior after the peak value of the stress. The 32.56-μm displacement was applied at the right side of the specimen and increased with every step.

Figures 5(a) and (b) show the axial stress distribution and crack propagations under static loading when m=5 and m=50, respectively. The stiffness matrix calculations become unstable when a finite element model is completely separated; thus, the calculations were stopped when the model specimens failed. Microcracks were initiated at many separate locations when m=5, while microcracks were generated densely at a location when m=50. The generated stress concentrations around the microcrack tips accelerated microcrack propagation, which led to specimen failure, in particular, the concentrations develop strongly

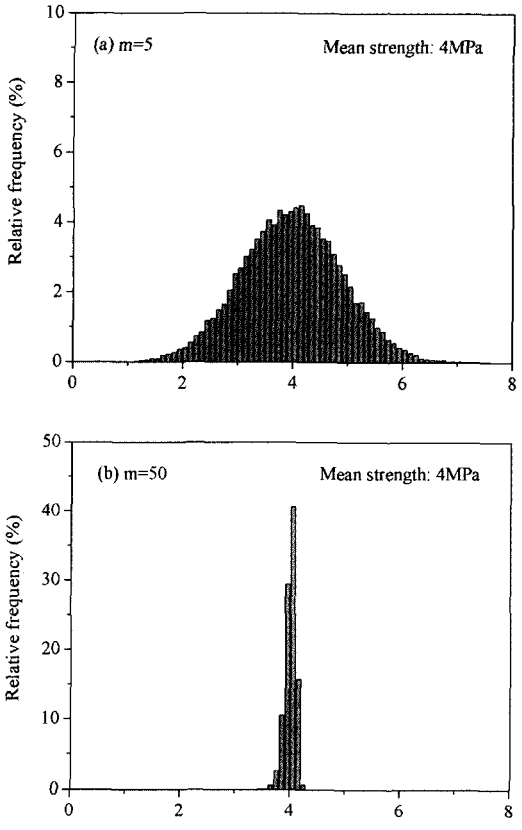

Fig. 4. Distribution of the microscopic tensile strength in the analysis model when (a) m=5, and (b) m=50

when m=50.

Figure 6(a) shows the complete stress-strain curve and the crack frequency when m=5. The cracking started when the stress was 1.60 MPa, and increased with the stress in the specimen. The specimen failed at the peak value of the curve, which was slightly higher than the minimum microscopic tensile strength shown in Fig. 4(a). The cracking frequency increased

rapidly near the peak value of the curve, and continued until the specimen failed. The cracking was related to acoustic emission (AE) events, which were caused by the release of elastic energy. To investigate the inhomogeneity effects on the static fracture process, a stress-strain curve with the crack frequency when m=50 is shown in Fig. 6(b). The curve contains a break after the peak value, *i.e.*, the curve shows a brittle response in the specimen. The crack generation frequency rapidly increased after the initiation of cracking near the peak value of the stress, and the specimen failed immediately after the peak value of the stress.

4. Determination of Static Tensile Strength

To determine the static tensile strength and the inhomogeneity effects, the fracture processes were simulated using specimens with ten different spatial microscopic strength distributions for m=5 and m=50.

Figures 7(a) and (b) show the crack patterns in specimens with different microscopic strength spatial distributions when m=5 and m=50. The figures just show five results when m=5 and m=50 respectively. The positions of the fracture plane varied with the microscopic strength spatial distribution.

The static tensile strengths were determined from the stress at the peak value of the stress-strain curve for each specimen models. Table 2 gives the static tensile

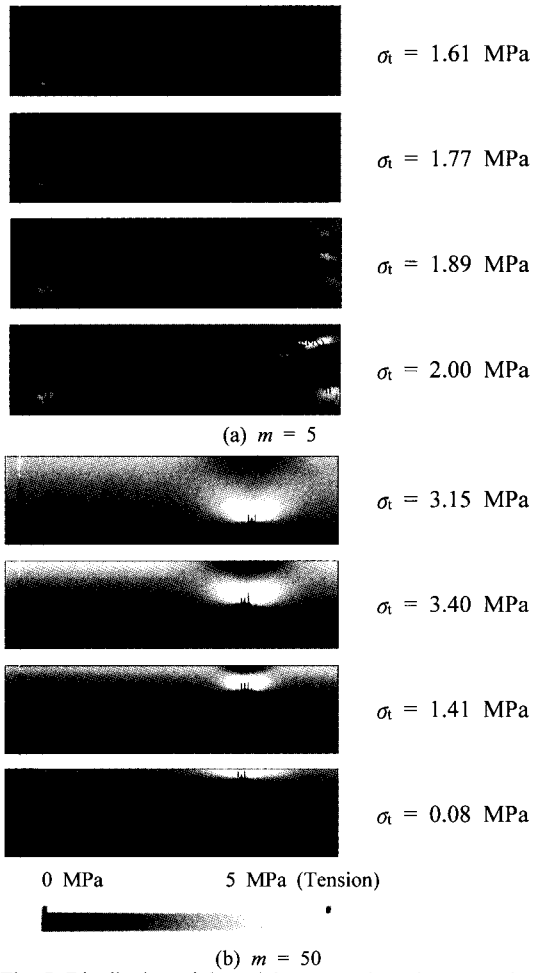

Fig. 5. Distribution of the axial stress and crack propagation under static loading when (a) m=5 and (b) m=50.

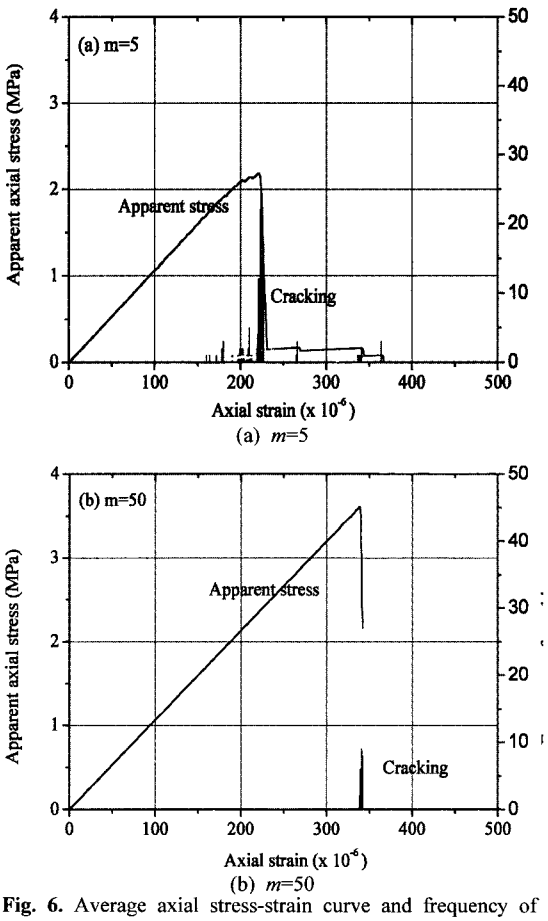

Fig. 6. Average axial stress-strain curve and frequency of cracking for static loading conditions: (a) m=5 and (b) m=50.

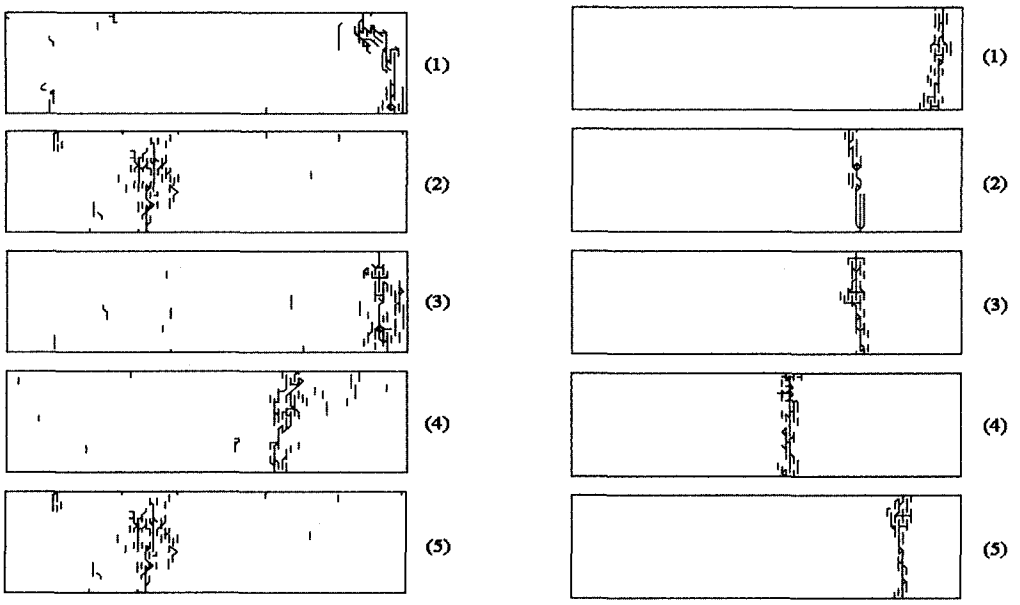

Fig. 7. Fracture and crack patterns with various spatial microscopic strength distributions when (a) m=5 and (b) m=50.

Table 2. Static tensile strength.

Length L (m)	Static tensile strength Ss (MPa)		
	m=5	m=50	m=∞
0.1	2.12±0.088	3.58±0.062	4
0.2	2.11±0.067	3.57±0.052	4

strengths of the specimens with ten different spatial microscopic strength distributions when m=5, m=50 and m= ∞. The mean values of the static tensile strength are 2.12±0.088 MPa when m=5 and 3.58± 0.062 MPa when m=50. These are slightly greater than the minimum microscopic strengths, and increase with the uniformity coefficient m. The tensile strength of the homogenous specimen, *i.e.* when m= ∞, was 4 MPa.

5. Influence of Rock Inhomogeneity and Discussion

Figures 8(a) and (b) show the distributions of static tensile strengths when m=5 and m=50. The static tensile strength becomes closer to the mean tensile strength at a higher uniformity coefficient and the

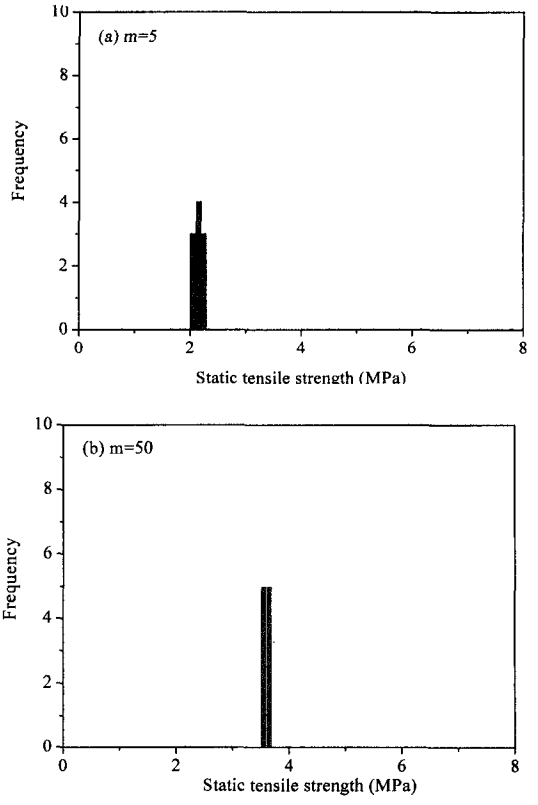

Fig. 8. Distribution of the static and dynamic tensile strengths when (a) m=5 and (b) m=50.

scatter of the strength data decreases with increasing uniformity coefficients. These results imply that rock inhomogeneity has an effect on static tensile strength and causes the scatter of static tensile strength.

When the static tensile strengths in Figs. 8(a) and (b) are compared with the microscopic tensile strengths in Figs. 4(a) and (b), the static tensile strengths are slightly higher than the minimum microscopic strength shown in Fig. 8(a), and are similar to the minimum microscopic strength shown in Fig. 8(b). We could realize that despite microfractures were generated with the applied stress correspond to the minimum microscopic strength, the failure of the specimen was generated with a little increasing of the applied stress when m=5. While when m=50 the failure of the specimen occurred under the applied stress correspond to the minimum microscopic strength. The cracking frequencies when m=5 and m=50 as shown in Figs. 6(a) and (b) support the fracture phenomena described above.

The scatter of the static tensile strength decreased with increasing uniformity coefficients as shown in Figs. 8(a) and (b). For this reason, we could point out the significantly different crack patterns in specimens with different spatial microscopic strength spatial distributions when m=5 and m=50 as shown in Figs. 7(a) and (b). These are related to microfractures and a failure caused by the microfractures. The microfractures are affected by the stress concentrations and redistribution mechanisms with respect to different spatial microscopic strength distribution as shown in Figs. 5(a) and (b). Therefore, it can be concluded that rock inhomogeneity has an effect on static tensile strength.

Additional calculations using the specimen of 0.2 m in length were carried out to investigate a variation of the static tensile strength with respect to a specimen size. The mean values of the static tensile strength were 2.08 ± 0.106 MPa in m=5 and 3.52 ± 0.053 MPa in m=50 as listed in Table 2. The mean static tensile strength increased with length increasing of specimen. It was confirmed that the analysis approach proposed could be capable to the fracture simulation considering the size effect of a specimen.

6. Conclusion

The fracture processes under static loading in tension were analyzed using a proposed finite element method to verify the influence of rock homogeneity on static tensile strength. Static tensile strengths were estimated in specimens with different spatial microscopic tensile strength when m=5 and m=50. The mean values of the static tensile strengths were 2.12 ± 0.088 MPa when m=5 and 3.58 ± 0.062 MPa when m=50. These were slightly greater than the minimum microscopic strengths, and increased with the uniformity coefficient m. The tensile strength of the homogenous specimen was 4 MPa. The static tensile strength became closer to the mean microscopic tensile strength, 4 MPa at a higher uniformity coefficient and the scatter of the strength data decreased with increasing uniformity coefficients. It was concluded that rock inhomogeneity has an effect on static tensile strength.

Acknowledgment

The authors wish to thank their research assistants, Mr. Kato Massaji for his helpful discussion.

References

1. Bacon, L. 1962, A method of determining dynamic tensile strength of rock at minimum loading. USBMRI 6067, 22.
2. Birkimer, D.L. 1970, A possible fracture criterion for the dynamic tensile strength of rock. Proc. 12th Symp. Rock Mech., Rolla, Missouri, 573-590.
3. Cho, S.H., Nohara, S., Kato, M., Ogata, Y., and Kaneko, K., 2002, Study on the strain-rate dependency of the dynamic tensile strength of rock. Proc. 7th Int. Symp. Rock Frag. Blast. Beijing, China, 144-150.
4. Cho, S.H., Hyung Sik Yang and Kaneko, K., Influence of rock inhomogeneity on the dynamic tensile strength of rock. J. of Korean Society for Rock Mech. (submitted)
5. Hillerborg, A. 1972, Application of the fictitious crack model to different materials. Int. J. Fracture, 51: 95-102.
6. Jung, W. J., Ogata, Y., Wada Y., Seto, M., Katsuyama, K. and Ogawa, T. 2001, Effects of water saturation and strain rate on the tensile strength of rocks under dynamic load. J. Geotech. Eng. JSCE, No. 673; III-54, 53-59 [in Japanese].
7. Kaneko, K., Matsunaga, Y., and Yamamoto, M. 1995, Fracture mechanics analysis of fragmentation process in

rock blasting. J. Jpn Explosive Society, 58(3): 91-99 [in Japanese].
8. Ma, G., Miyake, A., Ogawa, T., Wada, Y., Ogata, Y., Seto, M., and Katsuyama, K. 1998, Study on the tensile strength of brittle materials under high stress rate using the technique based on Hopkinson's effect. J. Jpn Exp. Soc., 59(2): 49-56 [in Japanese].
9. Reinhardt, H.W., Kormeling, H.A., and Zielinski, J.A. 1986, The split Hopkinson pressure bar, a versatile tool for impact testing of concrete. Mater. Struct., 19-55.
10. Rinehardt, J.S. 1965, Dynamic fracture strength of rocks. Proc. 7th Symp. Rock Mech., Univ. Park, Penn., 205-208.
11. Tedesco, J.W., Ross, C.A., and Kuennen, S.T. 1993, Experimental and numerical analysis of high strain rate splitting tensile tests. ACI Mater. J., 90: 162-169.
12. Weibull, W. 1951, A statistical distribution function of wide applicability. J. Appl. Mech., 18: 293-297.
13. Whittaker, B.N., Singh, R.N., and Sun, G. 1992, Rock fracture mechanics. Principles, Design and Application Elsevier.

조 상 호

1998년 전북대학교 자원공학과, 공학사
2000년 전남대학교 자원공학과, 공학석사

Tel: +81-11-706-6325
E-mail: chosh@geo-er.eng.hokudai.ac.jp
현재 북해도대학 대학원공학연구과, 박사과정

金子 勝比古

1970년 교토대학 자원공학과 공학사
1972년 교토대학 대학원공학연구과 공학석사
1986년 교토대학 대학원공학연구과 공학박사

Tel: +81-11-706-6322
E-mail: kaneko@geo-er.eng.hokudai.ac.jp
현재 북해도대학 대학원공학연구과, 교수

양 형 식

1979년 서울대학교 자원공학과 공학사
1981년 서울대학교 대학원 자원공학과 공학석사
1987년 서울대학교 대학원 자원공학과 공학박사
Tel: 062)530-1724
E-mail: hsyang@chonnam.ac.kr
현재 전남대학교 건설지구환경공학부 교수